Etch Characteristics of TiO$_2$ Etched by Using an Atomic Layer Etching technique with BCl$_3$ Gas and an Ar Neutral Beam

Jae Beom PARK and Woong Sun LIM

Sungkyunkwan Advanced Institute of Nano Technology (SAINT), Sungkyunkwan University, Suwon 440-746

Sang Duk PARK and Byoung Jae PARK

Department of Advanced Materials Engineering, Sungkyunkwan University, Suwon 440-746

Geun Young YEOM*

The National Program for Tera-level Nanodevices, Seoul 136-791

The etch characteristics of TiO$_2$ etched by using an atomic-layer-etching technique (ALET) with a BCl$_3$/Ar neutral beam were investigated. In addition, the surface composition after the etching by using the ALET was compared with that after the etching by using an inductively coupled plasma (ICP). By supplying BCl$_3$ gas at partial pressures >0.16 mTorr and by using Ar beam irradiation at doses >1.49 × 10^{17} atoms/cm^2·cycle, we could obtain a saturated etch rate of 1.25 Å/cycle (one monolayer /cycle). Therefore, by adjusting the number of etch cycles, we could control the etch depth with atomic precision. When the surface compositions of TiO$_2$ after etching by using ALET and by using an ICP were compared, no change of the surface composition was observed for the sample surface after the ALET while a Ti-rich surface was observed after the ICP etching.

I. INTRODUCTION

As the dimensions of integrated circuit devices, such as metal-oxide-semiconductor field effect transistors (MOS-FETs), *etc.*, continue to be scaled down, the thickness of gate dielectrics, such as SiO$_2$, *etc.*, also continues to be scaled down to nanosize [1]. Tunneling currents through the gate dielectric, however, limit the scaling of SiO$_2$ to approximately a few nanometers. Therefore, for further scaling down of devices, alternate gate dielectric materials with higher dielectric constants need to be used to reduce the gate leakage current while maintaining the gate-dielectric capacitance with a thicker material [2]. Among the various high-dielectric-constant materials, materials such as Al$_2$O$_3$, HfO$_2$, ZrO$_2$ and TiO$_2$ have been extensively studied to replace SiO$_2$. Especially, titanium dioxide, TiO$_2$, has been investigated over the years due to its high refractive index and high optical transmittance in the visible and near-IR regions, in addition to its high dielectric constant (∼100), for potential applications to capacitors in planar circuit construction, optical waveguides, electrodes for electrochemistry, *etc.* [3–9,20, 21]. In order to apply TiO$_2$ to MOSFET devices as a

gate dielectric, TiO$_2$ films should be patterned by reactive ion etching (RIE) for fine line delineation. Also, in manufacturing processing of nanoscale MOSFET devices, especially for gate-oxide etching processing, a precise control of the etch rate (depth) is required during etching, instead of a high etch rate, due to the extremely low thickness of the gate dielectric material. In addition, for gate dielectric processing of nanoscale devices, no damage on the etched surface is essential. However conventional RIE tends to cause electrical and physical damage to the surface of the devices due to use of energetic reactive ions and the difficulty in precise etch rate (depth) control on an atomic scale. For the etching of TiO$_2$ gate dielectrics in nanoscale MOSFET devices, an atomic-layer etching technique (ALET) may be the most suitable method because it is known to etch materials with atomic scale etch controllability and without etch damage [10]. Therefore, in this study, the etch characteristics of TiO$_2$ thin films etched by using ALET with BCl$_3$ for applications to nanoscale MOSFET devices were investigated. Especially, in this ALET for etching TiO$_2$, a neutral beam, instead of an ion beam, was used to avoid possible charge-related damage [11].
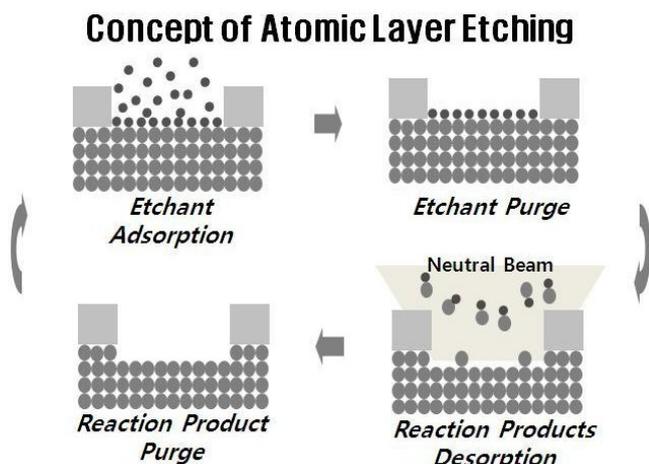
*E-mail: gyyeom@skku.edu; Fax: +82-31-299-6565

Concept of Atomic Layer Etching

Fig. 1. Concept of ALET processing composed of four steps.

Fig. 2. TiO$_2$ etch rate (Å/cycle) and RMS roughness when using ALET as functions of the BCl$_3$ gas pressure. the process conditions are an ICP source power of 300 W, a 1st grid voltage of +60 V, a 2nd grid voltage of –250 V, an Ar neutral-beam irradiation dose of 1.49 × 10^{17} atoms/cm^2·cycle and a reactant gas supply time of 20 s.

II. EXPERIMENTAL AND DISCUSSION

Figure 1 shows the concept of the ALET used in this experiment. Etching by using ALET is composed of four steps. The first step is the adsorption step in which an etch gas is introduced to the chamber and the etch gas is adsorbed (chemisorbed) on the sample surface. In this experiment, the etch gas was introduced for 20 s. The second step is the evacuation step in which remaining etch gas in the chamber is removed. The time for the second step was maintained at 3 s. The third step is the desorption step in which the chemisorbed molecules (reaction products) are removed from the sample surface by energetic particle bombardment. The last step is the evacuation step for the removal of reaction products from the chamber. The evacuation time was maintained at 3 s. A 100 nm-thick TiO$_2$ thin film deposited on a (100) silicon wafer by reactive sputtering and patterned by using a photoresist was used as a samples. In this experiment, BCl$_3$ was used as the etch gas for the adsorption step and an Ar neutral beam was used, instead of an Ar ion beam, for the desorption of the reaction products to avoid possible charge-related damage. The Ar neutral beam was formed by reflecting ions extracted from a three-grid ICP-type ion gun on a reflector that had parallel flat surfaces having a low angle (5°) to the ion beam direction [11]. For the operation of the ICP ion gun, a 300-W 13.56-MHz rf power was applied to the ICP source while supplying 30 sccm of Ar gas. To extract ions with energies about 60 eV, we applied +60 V to the acceleration grid located close to the ICP source; –250 V was applied to the extraction grid and 0 V was applied to the third grid located close to the reflector. The degree of neutralization of this neutral beam source was measured to be higher than 99 % [12–14]. To measure the etch depth, we used a step profilometer (Tencor Instrument, Alpha Step 500); then, we calculated the etch rate (etch depth/cycle) by dividing total etch depth by
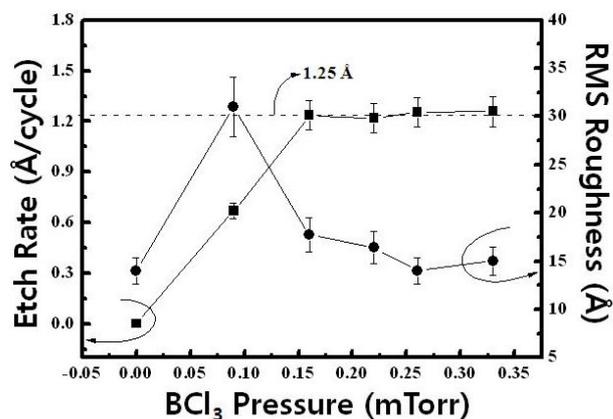
the number of etch cycles. The RMS surface roughness after etch process was measured using atomic force microscopy (Thermomicroscope, CP Research). The surface composition was measured using X-ray photoelectron spectroscopy (XPS, Thermo VG, MultiLab 2000, Mg K source).

Figure 2 shows the etch rate (Å/cycle) and RMS roughness (Å) of the TiO$_2$ for ALET measured as functions of the BCl$_3$ pressure during the adsorption step. The BCl$_3$ pressure was varied from 0 to 0.35 mTorr. The Ar neutral beam irradiation dose was kept at 1.49 × 10^{17} atoms/cm^2·cycle. As shown in the figure, when the BCl$_3$ gas pressure was increased from 0 to 0.16 mTorr, the etch rate of TiO$_2$ increased with increasing BCl$_3$ gas pressure and an etch rate of 1.25 Å/cycle was obtained at 0.16 mTorr; with further increases in the BCl$_3$ gas pressure, the etch rate saturated. In the case of the RMS surface roughness, increasing the BCl$_3$ gas pressure from 0 to 0.09 mTorr increased the RMS surface roughness from 13 to 31 Å, however; increasing the BCl$_3$ gas pressure higher than 0.09 mTorr decreased the surface roughness. Especially, for BCl$_3$ gas pressures higher than 0.26 mTorr, the RMS surface roughness decreased to 14 Å, which is close to the RMS surface roughness of the as-received TiO$_2$. The change in the etch rate (Å/cycle) with increasing BCl$_3$ gas pressure observed in the figure is related to the coverage (θ) of BCl$_3$ molecules on the TiO$_2$ surface. The θ of BCl$_3$ on the TiO$_2$ surface increases with increasing pressures and when the operating pressure is higher than a critical pressure, which is 0.16 mTorr, all of TiO$_2$ surface is covered with BCl$_3$, so the θ remains 1.0 even when the BCl$_3$ pressure is increased further [15]. Therefore, the etch rate increased with increasing BCl$_3$ gas pressure until the critical pressure for full surface coverage is reached and further increases in the BCl$_3$ pressure saturated the etch rate because the
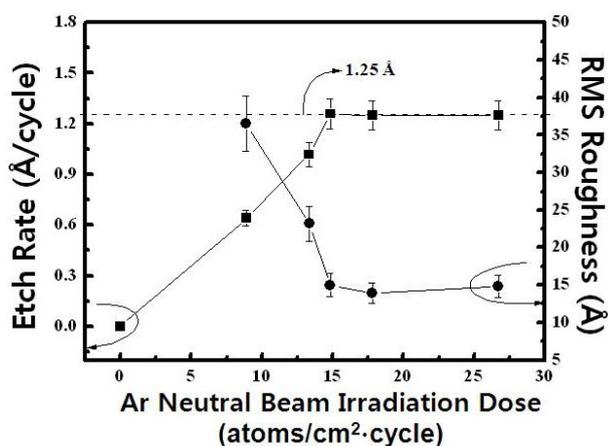
Fig. 3. TiO$_2$ etch rate (Å/cycle) and RMS roughness when using ALET as functions of the Ar neutral-beam irradiation dose. The process conditions are an ICP source power of 300 W, a 1st grid voltage of +60 V, a 2nd grid voltage of −250 V, a BCl$_3$ gas partial pressure of 0.33 mTorr and a BCl$_3$ gas supply time of 20 s.

coverage remained unchanged. The change in the RMS surface roughness is also related to the θ of the BCl$_3$ on TiO$_2$ surface. The initial increase in the BCl$_3$ pressure increases the θ of BCl$_3$ on the TiO$_2$ surface, but only a portion of the surface is covered with BCl$_3$, so only a portion of the surface layer is removed during the desorption step of each cycle. Therefore, an initial increase in θ increases the surface roughness. However, when the θ is higher than 0.5, that is, when BCl$_3$ is higher than 0.09 mTorr, more than half of the surface layer is removed during the desorption step. Therefore, at the pressures higher than 0.09 mTorr, the RMS surface roughness decreases with increasing operating pressure. When the θ becomes 1.0, one surface layer is removed during the desorption step of each cycle, so the surface roughness becomes close to that of the as-received TiO$_2$. During the adsorption step, the introduced reactive gas needs to react with the TiO$_2$ surface atoms and to form a volatile compound, which will be removed during the desorption step. If Cl$_2$ gas is used, instead of BCl$_3$ gas, as the reaction gas during the adsorption step of TiO$_2$ ALET, no etching is observed because no reaction compound is formed during the adsorption step. The bonding energy of Cl-O is 2.82 eV [16] while that of Ti-O is 6.98 eV [16]. Therefore, Cl$_2$ cannot react with TiO$_2$ and form volatile compounds such as TiCl$_x$ by removing oxygen from TiO$_2$. However, when BCl$_3$ gas (bonding energy of B-Cl is 5.56 eV [17]) is used as the reaction gas during the adsorption step, because the binding energy of B-O is 8.39 eV [16], which is higher than the binding energy of Ti-O, TiO$_2$ is dissociated and volatile TiCl$_x$ (binding energy of Ti-O : 5.13 eV [16]), which will be removed during the desorption step, is formed.

Figure 3 shows the etch rate (Å/cycle) and the RMS roughness measured as functions of the Ar neutral beam

irradiation dose during the desorption step. The Ar beam irradiation dose was increased from 0 to 2.7×10^{17} atoms/cm^2·cycle while BCl$_3$ gas pressure was maintained at 0.33 mTorr, which is higher than the critical pressure for $\theta = 1.0$. Increasing the Ar neutral beam irradiation dose from 0 to 1.49×10^{17} atoms/cm^2·cycle increased the TiO$_2$ etch rate and when the irradiation dose was higher than 1.49×10^{17} atoms/cm^2·cycle, the TiO$_2$ etch rate was saturated at an etch rate of 1.25 Å/cycle. In the case of RMS surface roughness, increasing the Ar neutral beam irradiation dose decreased the surface roughness continuously and when the irradiation dose was higher than 1.78×10^{17} atoms/cm^2·cycle, the surface roughness reached a minimum and did not change with further increases in the irradiation dose. The minimum surface roughness obtained was close to the surface roughness of the as-received TiO$_2$. The increase in the etch rate with the initial increase in the Ar neutral beam irradiation dose is related to the removal of a volatile compound formed on the TiO$_2$ surface. Because the BCl$_3$ gas pressure is higher than the critical pressure for $\theta = 1.0$, the entire TiO$_2$ surface is covered with one monolayer of the volatile compound. Therefore, the etch rate increases with increasing beam irradiation dose, which removes the volatile compound formed on the TiO$_2$ surface. However, when all of the volatile compound is removed by using the Ar neutral beam irradiation at a dose higher than the critical dose of 1.49×10^{17} atoms/cm^2·cycle, no volatile compound remains on the TiO$_2$ surface. Therefore, further increases in the irradiation dose do not increase the etch rate if the energy of the Ar neutral beam is less than the sputtering threshold of TiO$_2$ [18]. When the energy of the Ar neutral beam was about 60 eV, no sputtering of TiO$_2$ was observed while TiCl$_x$ was etched during the ALET. Therefore, saturation of the etch rate with increasing of Ar neutral beam irradiation dose could be obtained by using an adequate energy for the Ar neutral beam. The decrease in the RMS surface roughness with increasing Ar neutral beam irradiation dose is also related to the further removal of the volatile compound on the TiO$_2$ surface during each cycle. When the irradiation dose is higher than the critical dose to remove the entire volatile compound formed on the TiO$_2$ surface, the surface roughness becomes close to that of the as-received TiO$_2$ (13.9 Å) because one surface layer of TiO$_2$ is removed during each cycle. From Figures 2 and 3, both an operating pressure higher than the critical BCl$_3$ pressure for monolayer surface coverage of a reactive gas during the adsorption step and an Ar neutral beam irradiation dose higher than the critical dose for removal of all the volatile compound formed on the TiO$_2$ surface during the desorption step are required to obtain a one-monolayer etch rate of TiO$_2$ when using the ALET. If both process parameters are satisfied, the etch rate (Å/cycle) is maintained at 1.25 Å/cycle and the surface roughness remains similar to that of the as-received TiO$_2$.

Figure 4 shows the etch depth (Å) and the RMS surface roughness of TiO$_2$ measured as functions of the num-
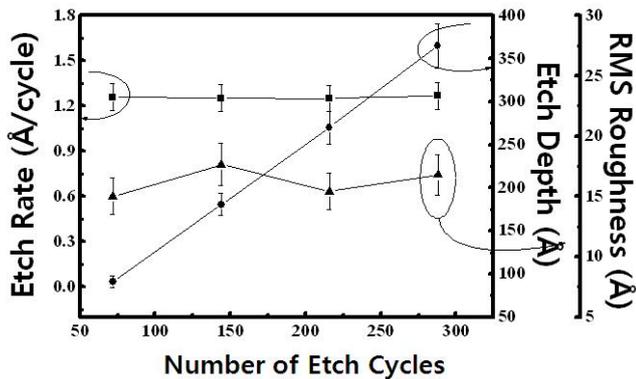
Fig. 4. Etch depth and etch rate (Å/cycle) of TiO$_2$ and RMS roughness when using ALET as functions of the number of etch cycles. The process conditions are an ICP source power of 300 W, a 1st grid voltage of +60 V, a 2nd grid voltage of −250 V, an Ar neutral-beam irradiation dose of 1.49 × 10^{17} atoms/cm^2 cycle, BCl$_3$ pressure of 0.33 mTorr and a BCl$_3$ gas supply time of 20 s.

ber of ALET etch cycles. The BCl$_3$ gas pressure and the Ar neutral beam irradiation dose were maintained at 0.33 mTorr and 1.49 × 10^{17} atoms/cm^2·cycle, respectively. As shown in the figure, the etch depth increased linearly with increasing number of etch cycles while maintaining an etch rate of exactly 1.25 Å/cycle. Also, the surface roughness remained between 15 and 17.6 Å, similar to that of the as-received TiO$_2$. Therefore, by controlling the number of etch cycles, an etch depth with atomic scale precision can be obtained by using ALET. In general, after RIE, the surface composition is modified due to the differences in the volatility of the reaction compounds formed on the etch material. Therefore, the surface composition after the etching was compared for an ALET and an ICP etching.

Figure 5 shows the surface composition of the TiO$_2$ surface measured by using XPS after an etching by using the ALET and an ICP etching. For the ALET, the etch condition shown in Figure 4 was used and for the ICP etching, a 300-W 13.56-MHz rf power and a −200 V bias voltage were used at an 8-mTorr operating pressure and the gas composition were Ar (20 sccm)/BCl$_3$ (60 sccm). The etch depth for both cases was maintained at about 100 Å. As shown in the figure, the ratio of Ti/O of the as-received TiO$_2$ was 0.554 while those of the TiO$_2$ surfaces after the ALET and the ICP were 0.559 and 0.599, respectively. In the case of ICP etching by Ar/BCl$_3$, due to the formation of a more volatile compound of BCl$_x$O$_y$ compared to TiCl$_x$ on the TiO$_2$ surface, the oxygen of the TiO$_2$ surface is preferentially removed during the etching by BCl$_3$ [19]. Therefore, the ratio of Ti/O becomes higher than that of the as-received TiO$_2$ after the etching. However, in the case of the ALET, due to the removal of one surface layer during each cycle, the ratio of Ti/O remains similar to that of the as-received TiO$_2$.
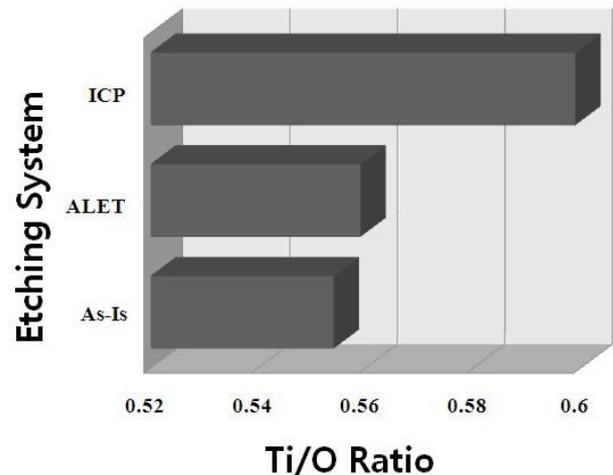

Fig. 5. Ti/O ratio measured using XPS for etching by using the ALET and an ICP. The process conditions for the ALET are the same as there in Figure 4. The ICP etching condition are an ICP power of 300 W, a dc bias voltage of −200 V, a BCl$_3$ gas supply of 60 sccm, an Ar flow of 20 sccm and a working pressure of 8 mTorr.

III. CONCLUSIONS

TiO$_2$ thin films that can applied as the gate dielectric material for nanoscale MOSFET devices were etched by using the ALET with BCl$_3$ as the adsorption gas and with an Ar neutral beam for the desorption of reaction compounds and the etch characteristics of the TiO$_2$ thin films were investigated. When the BCl$_3$ pressure was higher than a critical pressure (>0.16 mTorr) during the adsorption step and the Ar neutral beam irradiation dose was higher than a critical dose (>1.49 × 10^{17} atoms/cm^2) during the desorption step, a one-monolayer etch rate of TiO$_2$, that is, 1.25 Å/cycle could be obtained by using the ALET. In addition, the surface roughness after the etching by using ALET was similar to that of the as-received TiO$_2$. The critical BCl$_3$ pressure was related to the formation of full surface coverage with BCl$_3$ on the TiO$_2$ surface ($\theta = 1.0$) and the critical dose of the Ar neutral beam was related to the dose for the removal of all of the volatile compound formed on the TiO$_2$ surface. When the surface compositions were compared, the ratio of Ti/O after the ALET was similar to that of the as-received TiO$_2$ due to the complete removal of the surface layer during each cycle. We believe that the ALET can be applied to the etching of a gate dielectric material for next generation nanoscale MOSFET devices, which require precise etch depth, no etch damage, *etc.*

REFERENCES

[1] E. Y. Wu, E. J. Nowak, A. Vayshenker, W. L. Lai and D. L. Harmon, IBM J. Res. & Dev. **46**, 287 (2002).

[2] H. S. Kim, S. A. Campbell and D. C. Gilmer, IEEE Electr. Dev. Lett. **18**, 465 (1997).

[3] H. Kim, D. C. Gilmer, S. A. Campbell and D. L. Polla, Appl. Phys. Lett. **69**, 25 (1996).

[4] A. Fujishima and K. Honda, Nature **238**, 37 (1972).

[5] L. Forro, O. Chauvef, D. Emin, L. Zuppiroli, H. Berger and D. Levy, J. Appl. Phys. **78**, 1439 (2001).

[6] H. Tang, K. Prasad, R. Sanjinès, P. E. Schmid and F. Lévy, J. Appl. Phys. **75**, 2042 (1994).

[7] K. S. Lee, S. W. Jung, H. J. Son, K. S. Jang, J. I. Lee, H. J. Park, J. H. Kim, K. H. Kim and J. S. Yi, J. Korean Phys. Soc. **52**, 1863 (2008).

[8] K. D. Lee, J. Korean Phys. Soc. **52**, 1070 (2008).

[9] T. V. Chuong, L. Q. T. Dung and D. Q. Khieu, Korean Phys. Soc. **52**, 1526 (2008).

[10] Y. Zhang, Dry Process International Symposium **1-01**, 1 (2007).

[11] D. H. Lee, M. J. Chung, H. K. Hwang and G. Y. Yeom, Mater. Sci. Engin. C **23**, 221 (2003).

[12] B. J. Park, K. S. Min, S. D. Park, J. W. Bae, O. Vozniy and G. Y. Yeom, Solid State Phenomena **124**, 275 (2007).

[13] B. J. Park, S. W. Kim, S. K. Kang, K. S. Min, S. D. Park, S. J. Kyung, H. C. Lee, J. W. Bae, J. T. Lim, D. H. Lee and G. Y. Yeom, J. Phys. D: Appl. Phys. **41**, 024005 (2008).

[14] D. H. Lee, J. W. Bae, S. D. Park and G. Y. Yeom, Thin Solid Films **398**, 647 (2001).

[15] J. Ř. Čermáková, A. Marković, P. Uchytil and A. Seidel-Morgenstern, Chem. Eng. Sci. **63**, 1586 (2008).

[16] D. R. Lide, *CRC Handbook of Chemistry and Physics*, 3rd ed. (Chemical Rubber, Boca Raton, FL, 2000).

[17] R. F. Barrow, Trans. Faraday. Soc. **56**, 952 (1960).

[18] Y. Ayagi, K. Shinmaura, K. Kawasaki, K. Gamo and S. Namba, Thin Solid Films **225**, 120 (1993).

[19] S. D. Park, J. H. Lim, C. K. Oh, H. C. Lee and G. Y. Yeom, Appl. Phys. Lett. **88**, 094107 (2006).

[20] J. S. Kim, S. H. Hahn and E. J. Kim, J. Korean Phys. Soc. **51**, 2014 (2007).

[21] J. H. Park, M. A. Lee, Y. H. Kim, B. J. Park and H. J. Choi, J. Korean Phys. Soc. **53**, 50 (2008).